


Statistical Modeling and Optimization of Two-Layer Aluminum–Copper Pipe Fabrication by Friction Stir Welding

Mehdi Fallahati Naqibi¹ · Majid Elyasi¹  · Hamed Jamshidi Aval² · Mohammad Javad Mirnia¹

Received: 25 May 2021 / Accepted: 12 October 2021 / Published online: 8 November 2021
© The Indian Institute of Metals - IIM 2021

Abstract In this research, the process and geometric parameters in the fabrication of copper–aluminum double-layer pipe using friction stir welding have been optimized by Box–Behnken design of response surface methodology. This research aims to optimize the rotational and traverse speed of the tool as well as the diameter and thickness of the pipe to achieve the maximum tensile strength of the double-layer copper–aluminum pipe. In order to establish the relationship between input variables and joint strength, a quadratic model was used. The coefficients for the quadratic terms for the tool rotation speed and pipe thickness were considered to be very important, which shows that these parameters have a much greater effect on the joint strength. However, the effect of traverse speed and pipe diameter on joint strength is negligible in terms of linear and nonlinear effects. The composite desirability of the parameters is $D = 0.9168$. This desirability in the parameters of rotational speed, traverse speed, pipe diameter, and pipe thickness, which are 660 rpm, 80 mm/min, 24 mm, and 1.4 mm, respectively, has shown the joint strength of 341.86 MPa. Also, the average tensile strength measured from the experiments is 347.33 MPa, which is very close to the models' estimated value. The R^2 value after modifying the model indicates the 88% predictability of the model.

Keywords Double-layer aluminum–copper pipe · Response surface methodology · Joint strength

1 Introduction

The joining of dissimilar metals is an interesting idea in the industrial parts design and manufacturing industry. The purpose of joining two dissimilar metals is to combine the two metals' mechanical and thermal properties [1]. The production of dissimilar joints by conventional fusion welding methods is complicated and, in some cases, impossible due to the different melting point of two metals, extensive changes in the microstructure of the base material, the generation of residual stresses, and the formation of intermetallic compounds [2–4]. This extensive change in the properties of materials and the formation of intermetallic compounds causes the brittleness of the weld zone and reduces the strength of joints [5–7]. Solid-state welding is a useful technique for bonding such metals because in this technique, the bonding process takes place below the melting temperature of the two metals, as a result of the fact that oxidation does not occur and there is no need for shielding gas and consumables [8, 9]. In general, in solid-state processes, defects associated with melting-solidification phenomena are not present and unions as strong as the base material can be made [10, 11]. In these methods, the heat-affected zone (HAZ), which is the source of many defects and is one of the main reasons for reducing mechanical properties, is very small [12]. Friction stir welding (FSW) was first invented at the welding institute (TWI) in 1991. This fabrication method is a type of solid-state welding process first applied on aluminum alloys [13]. The joint in this method is achieved by friction between the

✉ Majid Elyasi
elyasi@nit.ac.ir; elyasima@yahoo.com

¹ Department of Mechanical Engineering, Babol Noshirvani University of Technology, Shariati Avenue, Babol 47148-71167, Iran

² Department of Materials Engineering, Babol Noshirvani University of Technology, Shariati Avenue, Babol 47148-71167, Iran

workpiece and a non-consumable tool resistant to wear and heat [14]. Today, many studies are done in relation to this process, which include examining the effect of various parameters on the joint area's properties. Studies have been performed on the bonding of dissimilar metals, especially the joining of aluminum to other metals, including copper. Barekatin et al. [15] investigated the joining of AA1050 aluminum alloy to pure copper. They stated that annealing heat treatment helps to increase the strength of the joint. According to the results of their work after heat treatment, the joint's failure point was transferred from the stir zone to the aluminum base metal. Argesi et al. [16], in a study on the weldability of two dissimilar metals, copper and aluminum, came to an important and interesting conclusion and stated that the presence of intermetallic compounds between these two metals has a negative effect on the joining of the two metals. They stated that the mechanical properties of joints greatly depend on grain size and intermetallic compound in the SZ. Celik and Cakir [17] controlled the heat input to the joint by changing the tool offset, diameter, rotational speed, and traverse speed of the tool. They concluded that by controlling the tool's geometric parameters and processing parameters, the joint's strength and elongation could be controlled. Liu et al. [18] investigated the formation of the layered structure in the SZ of the 5A06 aluminum and copper joint. They stated that the SZ structure near copper and aluminum sides is different while joining these two materials. In the copper side and aluminum side of SZ, a layered structure and mixed aluminum zone and copper formed, respectively. In a research study, Galvão et al. [19–21] investigated the effect of tool geometry and processing parameters on the formation and distribution of brittle intermetallic structures in FSW of aluminum and copper. They stated that tool geometry plays an important role in forming and distributing brittle intermetallic compounds.

In the field of FSW of circular sections, limited studies have been carried out by researchers [22–28]. Studies on FSW of circular sections in lap joining design are as follows: Jamshidi and Falahati [29] investigated the lap FSW process of AA5083-H321 aluminum pipe with a diameter of 360 mm to AA5083-O aluminum pipe with a diameter of 350 mm. In this study, the effect of tool rotational speed and pipe rotational speed in the FSW process was

investigated by tensile test and metallographically examination. Finally, the rotational speeds of 650 and 800 rpm and the traverse speed of 40 mm/min are introduced as the best parameters for welding in their study. Li et al. [30] investigated the production of two-layer aluminum–copper pipe by friction welding. Although they have successfully produced two-layer aluminum–copper pipes by friction welding process, the main problem of their procedure is the impossibility of performing the process in producing pipes with long lengths and large diameters. Tavassolimanesh and Alavi Nia [31] investigated the FSW of aluminum and copper pipes as a lap joint scheme. They examined only one weld line on the tube and did not examine the effect of joining parameters such as the overlap of different passes.

As mentioned, to investigate the effect of FSW parameters on the microstructure and mechanical properties of joints, some researchers use traditional methods, in which all parameters are considered constant, and only one parameter is changed. However, in this method, the interaction between the parameters is not considered, and they are not cost-effective in terms of time and cost. For this reason, this method is not a suitable method to obtain optimal parameters [32]. In recent years, researchers have used various optimization methods such as the Taguchi method, Response surface methodology (RSM), and Neural network to optimize the parameters affecting the FSW process [32–41]. The first step of the proposed approach for optimizing the parameters is to design an experiment. The purpose of this design is to obtain the maximum possible information with the least number of experiments. Through the design of the experiment, engineers identify the most important variables affecting processes and determine their optimal levels. An experiment is a set of planning efforts in which variables that are thought to affect goals are systematically changed, and the output of these changes (goal values) is recorded. There are several ways to perform these tests, including full and fractional factorial design. The main advantage of the full factorial design is obtaining information from all goal variables and their relationships. On the other hand, as the number of factors increases, the number of experiments increases exponentially, and the method's efficiency decreases. However, the fractional factorial design has the advantage that the data can be collected and analyzed with fewer experiments, leading to

Table 1 Chemical composition of AA5086 aluminum alloy and copper C12200

Alloy	Al	Ti	Zn	Cr	Mg	Mn	Cu	Fe	Si	P
AA5086	Base	0.15	0.25	0.25	4.5	0.7	0.1	0.5	0.4	–
C12200	–	–	–	–	–	–	Base	–	–	0.04

Fig. 1 Friction stir welding mechanism for fabrication of two-layer tube



Table 2 Parameters and levels considered in this study

Parameters	Coded	Un coded	Levels		
			Lower (- 1)	Middle (0)	Upper (1)
Rotating speed, (rpm)	x_1	X_1	400	600	800
Thickness of pipe, (mm)	x_2	X_2	1.0	1.5	2.0
Diameter of pipe (mm)	x_3	X_3	24	44	64
Traverse speed, (mm/min)	x_4	X_4	40	60	80

less cost and time. RSM is one of the most widely used methods to optimize variables in various sciences. RSM uses a combination of a series of mathematical and statistical models to examine the effect of different parameters on response variables. Also, it can create quadratic

regression equations to optimize response variables [42]. The RSM includes different design models such as central composite and Box–Behnken designs. The Box–Behnken method employs a quadratic model for three levels and has fewer tests than the central composite method. The surfaces

Table 3 Experiments presented by the Box–Behnken design method for four continuous variables

Sample no	U (rpm)	V (mm/min)	T (mm)	D (mm)
1	− 1	0	− 1	0
2	1	0	− 1	0
3	− 1	0	1	0
4	1	0	1	0
5	0	− 1	0	− 1
6	0	− 1	0	1
7	0	1	0	− 1
8	0	1	0	1
9	− 1	− 1	0	0
10	1	− 1	0	0
11	− 1	1	0	0
12	1	1	0	0
13	0	0	− 1	− 1
14	0	0	1	− 1
15	0	0	− 1	1
16	0	0	1	1
17	− 1	0	0	− 1
18	1	0	0	− 1
19	− 1	0	0	1
20	1	0	0	1
21	0	− 1	− 1	0
22	0	− 1	1	0
23	0	1	− 1	0
24	0	1	1	0
25	0	0	0	0
26	0	0	0	0
27	0	0	0	0

are arranged from bottom to top, and the center number is known as the center point. Bottom, center, and top points are coded with -1 , 0 , and 1 , respectively. Although various optimization methods are used to optimize the parameters affecting the FSW process, limited research has been done in optimizing pipe FSW. Senthil et al. [43] used the RSM method to optimize process parameters in the FSW of AA6063 aluminum alloy pipes. They reported that by considering the desirability function method, the maximum strength and elongation are obtained in FSW of AA6063 pipe with an outer diameter of 50 mm at a tool rotational speed of 1986 rpm and a pipe rotational speed of 0.65 rpm. Using the RSM-Fuzzy hybrid method, Kassas and Sabry [44] studied underwater FSW of AA1050 aluminum pipe. They selected the joint's tensile strength as a criterion for optimizing the parameters and showed that the method used by them predicts the results more accurately than the Artificial Neural Network method.

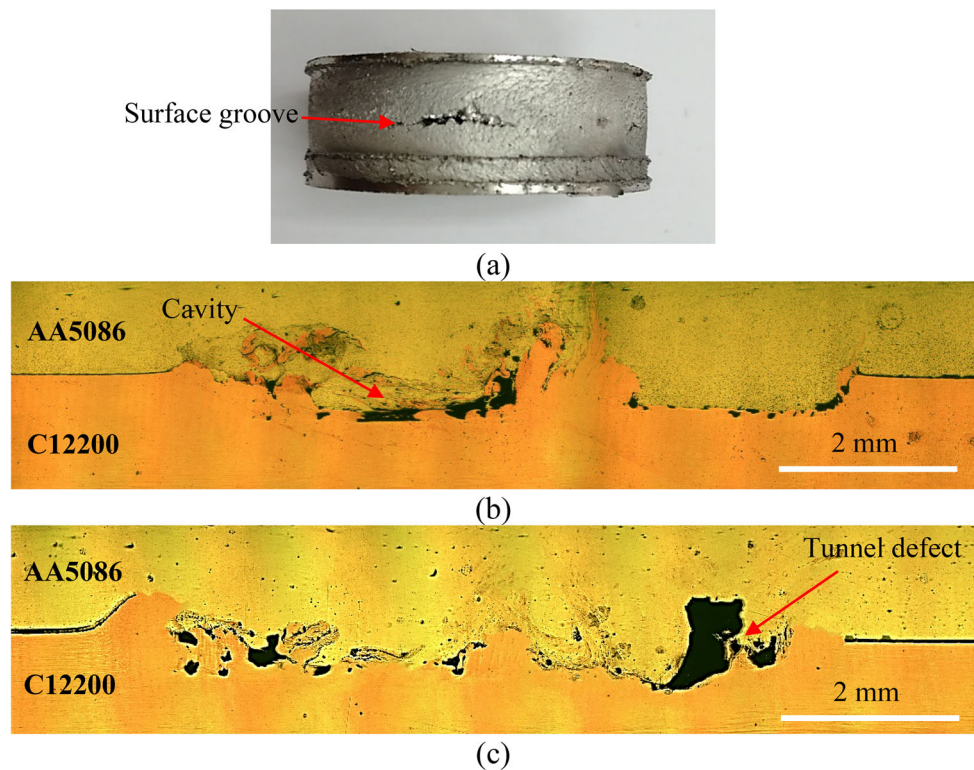
As it is clear from reviewing various researches, no research has been done in optimizing the parameters of the FSW process in the construction of copper–aluminum

double-layer pipes. Since process parameters such as rotational speed, traverse speed, and overlap of different passes as well as geometric parameters of pipe such as pipe diameter and thickness strongly affect the mechanical properties of the joint, optimization of process and geometric parameters in fabrication of the two-layer copper–aluminum pipe using FSW seems necessary to achieve maximum joint strength. Therefore, in this study, using RSM -based desirability function approach, process and geometric parameters were optimized to achieve a maximum tensile strength of the joint in the construction of AA5086 aluminum/C12200 copper double-layer pipe using FSW.

2 Experimental Procedure

In this research, AA5086 aluminum and C12200 copper alloys were, respectively, used for the outer and inner pipes with a length of 150 mm. The chemical composition of the two alloys is listed in Table 1. The inner diameters of the

Fig. 2 Defects formed during fabrication of double-layer Al/Cu pipe using FSW; **a** surface groove at top surface of welded sample with rotational speed 400 rpm, traverse speed 80 mm/min, pipe thickness 1.5 mm, and pipe diameter 44 mm, **b** cavity at weld cross section in the welded sample with rotational speed 400 rpm, traverse speed 40 mm/min, pipe thickness 1.5 mm, and pipe diameter 44 mm, **c** tunnel defect at weld cross section in welded sample with rotational speed 800 rpm, traverse speed 40 mm/min, pipe thickness 1.5 mm, and pipe diameter 44 mm



aluminum and copper pipes were 24–64 mm and 22–63 mm, respectively, while both had a thickness of 1–2 mm. The designed set shown in Fig. 1 was used to perform welding. The set included a cylindrical pin tool with a shoulder to pin diameter (D/d) ratio of 3 and pin heights of 1.3, 1.8, and 2.3 mm for pipes with thicknesses of 1, 1.5, and 2 mm, respectively. The thickness of the Al and Cu pipes was considered the same. A tilt angle of 3° was considered during friction stir welding. As presented in Table 2, the process and geometric parameters considered in the study included rotational speed, traverse speed, pipe diameter, and thickness. Based on the authors' initial studies on the overlap of different passes, it was found that the highest joint strength was achieved by 0.5 mm overlapping of SZ of two passes. Therefore, the same value was used for different passes in the current study. After FSW, the welded samples were cut perpendicular to the welding direction to investigate the microstructure. After grinding and polishing, the modified Poulton's solution containing two different solutions, i.e., (25 ml of nitric acid, 1 g of chromic acid dissolved in 12 ml of water) and (12 ml of hydrochloric acid, 6 ml of nitric acid, 1 ml of fluoric acid, and 1 ml of water), was used for etching the aluminum alloy. A solution of 50 ml HNO_3 and 50 ml H_2O was also utilized to etch the copper alloy. A more detailed study of microstructural changes was performed on the samples by scanning electron microscopy (SEM). The mechanical properties of the welded samples were measured by

conducting a ring tensile test and a ring hoop tension test (RHHT). The RHHT was performed according to the procedure reported in [45].

3 Model Development

The number of experiments required to use the Box–Behnken design method is defined as Eq. (1) [46]:

$$N = 2K(K - 1) + C_0 \quad (1)$$

where K is the number of input parameters, and C_0 is the number of central points. In this research, the purpose of test design is to model and optimize experimental conditions for achieving maximum ultimate tensile strength (UTS) of the joint. Four main factors, including rotational speed, traverse speed, the inner diameter of aluminum pipe, and aluminum pipe thickness, were selected as continuous variables at three levels. It should be noted that the thickness of the Al and Cu pipes was the same in each case. The central point of the design for estimating errors was repeated three times. Table 2 provides the upper and lower levels of the parameters. The relationship between input parameters and output parameter is expressed in Eq. (2) [46]:

$$\text{Strength} = f(X_1, X_2, X_3, X_4) \quad (2)$$

The mathematical relationship between coded variables

Table 4 Measured strength of welded samples under different factors

Sample no	U (rpm)	V (mm/min)	T (mm)	D (mm)	Strength (MPa)
1	-1	0	-1	0	230.67
2	1	0	-1	0	245.16
3	-1	0	1	0	226.14
4	1	0	1	0	275.13
5	0	-1	0	-1	219.93
6	0	-1	0	1	312.39
7	0	1	0	-1	337.89
8	0	1	0	1	229.12
9	-1	-1	0	0	250.78
10	1	-1	0	0	225.86
11	-1	1	0	0	220.12
12	1	1	0	0	329.21
13	0	0	-1	-1	238.96
14	0	0	1	-1	265.12
15	0	0	-1	1	263.98
16	0	0	1	1	239.12
17	-1	0	0	-1	259.23
18	1	0	0	-1	212.05
19	-1	0	0	1	216.46
20	1	0	0	1	321.57
21	0	-1	-1	0	254.18
22	0	-1	1	0	284.96
23	0	1	-1	0	272.43
24	0	1	1	0	241.45
25	0	0	0	0	309.34
26	0	0	0	0	308.12
27	0	0	0	0	310.95

and non-coded variables was determined based on the following equations [46]:

$$x_1 = \frac{X_1 - 600}{200}, \quad x_2 = \frac{X_2 - 1.5}{0.5}, \quad x_3 = \frac{X_3 - 44}{20}, \quad (3)$$

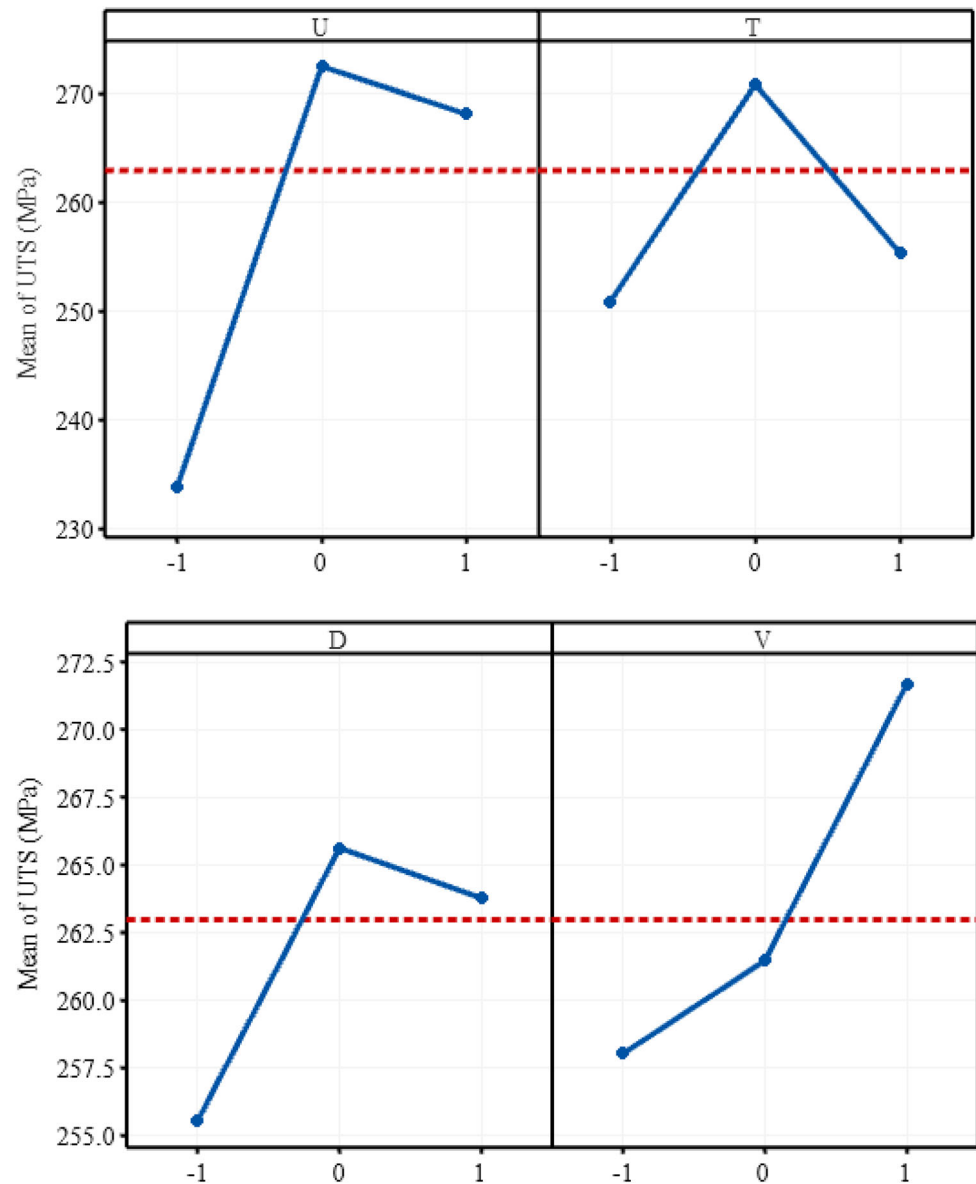
$$x_4 = \frac{X_4 - 60}{20}$$

In the presented relations, X_1 , X_2 , X_3 , and X_4 are unencoded variables. Besides, x_1 , x_2 , x_3 , and x_4 are encoded variables. According to the relations, it is clear that the unencoded variables retain their original unit, while the encoded variables are dimensionless. The model used in the RSM is a quadratic polynomial equation. In the RSM, a model is defined for each dependent variable that expresses the factors' main and interaction effects on each separate variable. The multivariate model is as follows:

$$Y = \beta_0 + \sum_{i=1}^K \beta_i x_i + \sum_{i=1}^K \beta_{ii} x_i^2 + \sum_{i < j}^K \beta_{ij} x_i x_j + \varepsilon \quad (4)$$

In this equation, Y is the predicted response, β_0 is the coefficient of interception, β_i is the linear coefficient, β_{ii} is the square coefficient, and β_{ij} is the interaction coefficient. Moreover, x_i are independent variables, and ε is the random error value. Also, i and j are the index numbers of the variables, and x_i is the dimensionless coded variable of X_i . The symbols U , T , D , and V are used for the non-coded variables X_1 , X_2 , X_3 , and X_4 , respectively, which represent the rotational speed, pipe's thickness, pipe's inner diameter, and traverse speed, respectively. Regression coefficients were calculated by Minitab 19 software, and the model was calculated at a 95% confidence level. As presented in Table 3, the Box–Behnken design method presents 27 experiments for four continuous variables. In order to investigate the effect of process parameters on the responses, a three-dimensional diagram of the regression

Fig. 3 Diagrams of the main effects of the variables of rotational speed (U), traverse speed (V), thickness (T), and diameter (D) of pipe on the joint strength



equations is drawn to obtain the optimal values of the variables within the considered ranges.

4 Results and Discussion

According to preliminary studies performed on welded samples, two common types of defects have been observed in welded samples. As shown in Fig. 2, these defects include surface groove at the weld crown and cavity or tunnel defects at the weld cross section. According to previous studies [47–49], the surface groove defect occurs at insufficient heat input, and insufficient forging on the workpiece surface and the cavity or tunnel defects occur due to abnormal stirring of material in the SZ at excessive or insufficient heat input. The occurrence of any of these

defects will cause a decrease in the strength of the joint. It is necessary to know and consider these defects in analyzing the effect of different parameters on the strength of the joint.

As previously mentioned, to evaluate the effect of tool rotation speed, traverse speed, thickness, and pipe's diameter on the strength of joints, the Box–Behnken design was used based on the RSM. Initially, a mathematical model is created using the Box–Behnken method. This model is able to explain the relationships between parameters and their interaction to predict and control the strength of the joint using different parameters. Then, using analysis of variance (ANOVA), the effect of each parameter and the optimal conditions for joint strength will be expressed based on the parameters. The measured joint strength values from the experimental tests are presented in

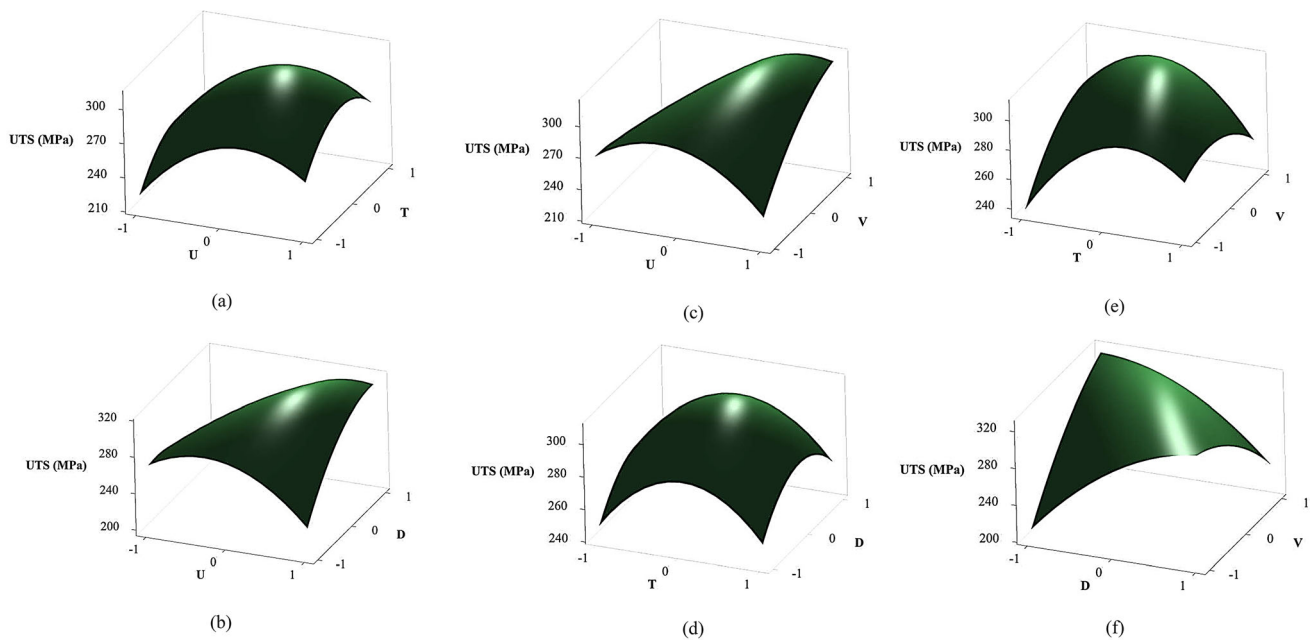


Fig. 4 Interaction effect of parameters on the joint strength; **a** the interaction between rotational speed (U) and pipe thickness (T), **b** the interaction between rotational speed (U) and pipe diameter (D), **c** the interaction between rotational speed (U) and traverse speed (V), **d** the interaction between pipe thickness (T) and pipe diameter (D), **e** the interaction between traverse speed (V) and pipe thickness (T), **f** the interaction between traverse speed (V) and pipe diameter (D)

Table 4. In order to establish the relationship between uncoded input variables and joint strength, a quadratic model was used as follows. It should be noted that multiplying two parameters means the interaction of these two parameters. For example, $U * T$ indicates the interaction of rotational speed and thickness.

$$\begin{aligned} \text{Strength (MPa)} = & 309.47 + 17.13U + 2.21T + 4.12D \\ & + 6.84V - 35.35U * U - 32.24T * T \\ & - 22.42D * D - 14.61V * V + 8.63U * T \\ & + 38.07U * D + 35.50U * V \\ & - 12.76T * D - 15.44T * V - 50.31D * V \end{aligned} \quad (5)$$

Figure 3 shows the diagrams of the main effects of the variables of rotational speed, traverse speed, thickness, and diameter of the pipe on the joint strength. The effect of traverse speed is positive so that with increasing traverse speed, the strength increases. The heat input during FSW can be predicted according to the Arbogast equation [50]:

$$\text{Heat input} = K \left(\frac{\omega^2}{v \times 10^4} \right)^\alpha \quad (6)$$

where ω and v are rotational and traverse speed, respectively. K and α are the constants related to the material. It can be seen that with increasing traverse speed, the heat input decreases. Reducing the heat input, on the one hand, reduces the flowability of the material in the stir zone and

thus increases the possibility of defect formation at the joint. On the other hand, reducing the heat input reduces the formation of brittle intermetallic compounds at the joint and prevents joint strength reduction [51–53]. According to the results, it can be expected that the positive effect of reducing the heat input on the joint strength by reducing the formation of intermetallic compounds has led to an increase in joint strength. As can be seen, the average tensile strength of the joint is minimum in the values of +1 and -1 of rotational speed, diameter, and thickness of the pipe and shows the maximum value in their middle. The decrease in strength at a rotational speed of 800 rpm can be related to the increase in heat input, resulting in increased formation of intermetallic compounds and brittleness of the joint [52, 54]. By increasing the thickness and diameter of the pipe to 2 mm and 64 mm, respectively, an increase in the heat sink at the joint and thus a decrease in the flowability of material at the SZ occur. Therefore, it can be expected that although the probability of formation of intermetallic compounds decreases in these conditions, due to improper flow of material in the SZ, the probability of defect formation in the SZ increases, and this can reduce the joint strength.

To investigate the effect of process parameters on joint strength, three-dimensional diagrams were drawn under certain conditions. In fact, it is a graphical representation of regression equations that is used to determine the optimal values of variables within a specified range. The graphs

Table 5 Analysis of variance results for the model

Source	Degree of freedom	Sum of squares	Mean squares	<i>F</i> value	<i>P</i> value
Model	14	36,106.0	2579.0	12.28	0.000
Linear	4	4346.5	1086.6	5.17	0.012
<i>U</i>	1	3521.9	3521.9	16.76	0.001
<i>T</i>	1	58.7	58.7	0.28	0.607
<i>D</i>	1	203.9	203.9	0.97	0.344
<i>V</i>	1	562.0	562.0	2.67	0.128
Square	4	9446.6	2361.6	11.24	0.001
<i>U</i> * <i>U</i>	1	6664.8	6664.8	31.72	0.000
<i>T</i> * <i>T</i>	1	5542.0	5542.0	26.38	0.000
<i>D</i> * <i>D</i>	1	2680.9	2680.9	12.76	0.004
<i>V</i> * <i>V</i>	1	1138.1	1138.1	5.42	0.038
Two-way interaction	6	22,313.0	3718.8	17.70	0.000
<i>U</i> * <i>T</i>	1	297.6	297.6	1.42	0.257
<i>U</i> * <i>D</i>	1	5798.1	5798.1	27.60	0.000
<i>U</i> * <i>V</i>	1	4489.7	4489.7	21.37	0.001
<i>T</i> * <i>D</i>	1	650.8	650.8	3.10	0.104
<i>T</i> * <i>V</i>	1	953.6	953.6	4.54	0.055
<i>D</i> * <i>V</i>	1	10,123.4	10,123.4	48.19	0.000
Error	12	2521.1	210.1		
Lack of fit	10	2517.1	251.7	124.92	0.008
Pure error	2	4.0	2.0		
Total	26	38,627.1			
$R^2 = 0.9347$	$R^2(\text{adj}) = 0.8586$	$R^2(\text{pred}) = 0.6244$			

show interactions between two variables, and the rest of the parameters are kept in the middle value. Figure 4a shows the interaction between rotational speed and pipe thickness on the joint strength. A simultaneous decrease in rotational speed and pipe thickness indicates the lowest strength. Figure 4b shows the interaction between the rotational speed and the diameter of the pipe on the joint strength. Increasing the rotational speed and decreasing the pipe diameter show the lowest strength. Figure 4c shows the interaction between rotational speed and traverse speed on the joint strength. By increasing the rotational speed and decreasing the traverse speed, the minimum strength of the joint is obtained. Figure 4d shows the interaction between the thickness and the diameter of the pipe on the joint strength. As can be seen in both the minimum and maximum diameter of the pipe, if the thickness of the pipe decreases or increases from the middle value, the minimum joint strength is obtained. Maximum joint strength is obtained when the middle value of thickness and diameter are selected. Figure 4e, f shows the interaction of thickness and diameter of the pipe with the traverse speed, respectively. It is observed that the minimum strength occurs when the traverse speed and the diameter of the pipe

increase or decrease simultaneously, and also when the traverse speed and the thickness of the pipe decrease or increase at the same time. Although the heat input decreases with decreasing rotational speed, the heat sink decreases with decreasing thickness. Therefore, it can be said that although the heat losses at the joint are reduced, the effect of reducing the heat input due to decreasing rotational speed is much greater, and this reduces the proper flow of material in the SZ. In other words, the heat input increases with increasing rotational speed and decreasing traverse speed [50], but the heat sink decreases with decreasing thickness and diameter of pipes. Therefore, it can be said that the heat entered at the joint is not easily lost, and this leads to a SZ with a high temperature. Therefore, it can be expected that abnormal stirring at the SZ as well as high temperature increases the likelihood of the formation of welding defects such as tunnel defects as well as intermetallic compounds at the joint. As a result, the joint strength can be reduced.

The results of the analysis of variance are presented in Table 5. Analysis of variance is an analytical method to determine the importance of the model and parameters. The R^2 coefficient is defined as the ratio of the created

Table 6 Analysis of variance results for the modified model

Source	Degree of freedom	Sum of squares	Mean squares	<i>F</i> value	<i>P</i> value
Model	12	35,157.7	2929.8	11.82	0.000
Linear	4	4346.5	1086.6	4.38	0.017
<i>U</i>	1	3521.9	3521.9	14.21	0.002
<i>T</i>	1	58.7	58.7	0.24	0.094
<i>D</i>	1	203.9	203.9	0.82	0.080
<i>V</i>	1	562.0	562.0	2.27	0.074
Square	4	9446.6	2361.6	9.53	0.001
<i>U</i> * <i>U</i>	1	6664.8	6664.8	26.89	0.000
<i>T</i> * <i>T</i>	1	5542.0	5542.0	22.36	0.000
<i>D</i> * <i>D</i>	1	2680.9	2680.9	10.82	0.005
<i>V</i> * <i>V</i>	1	1138.1	1138.1	4.59	0.050
Two-way interaction	4	21,364.7	5341.2	21.55	0.000
<i>U</i> * <i>D</i>	1	5798.1	5798.1	23.40	0.000
<i>U</i> * <i>V</i>	1	4489.7	4489.7	18.12	0.001
<i>T</i> * <i>V</i>	1	953.6	953.6	3.85	0.070
<i>D</i> * <i>V</i>	1	10,123.4	10,123.4	40.85	0.000
Error	14	3469.4	247.8		
Lack of fit	12	3465.4	288.8	143.32	0.507
Pure error	2	4.0	2.0		
Total	26	38,627.1			
$R^2 = 0.9102$	$R^2(\text{adj}) = 0.8332$	$R^2(\text{pred}) = 0.8896$			

change to the total change, which is a scale for predicting the model. In reference to predict a suitable model, a minimum value of R^2 of 0.8 has been suggested [55]. In this study, the R^2 value is 0.9347, and the adjusted value of R^2 is 0.8586. These values indicate that the proposed model has a very good reaction capability. On the other hand, the values of F and P for the model are equal to 12.28 and 0.000, respectively, which shows that the proposed model is very effective. It is stated in references [55] that the value of P less than 0.1 shows the effectiveness of the model statistically. However, if the value of P is more than 0.1, it indicates that the model is not effective. The F -test is to determine the significance of the regression coefficients using the standard P value. In general, higher F values and lower P values indicate the greater importance of the terms [56]. The coefficients for the quadratic terms for the tool rotation speed and pipe thickness have been realized to be very important, which shows that these parameters have a much greater effect on the joint strength. However, the effect of traverse speed and pipe diameter on joint strength is negligible in terms of linear and nonlinear effects. To express the interaction of the parameters, the maximum effectiveness is for traverse speed and pipe diameter, tool rotation speed and pipe diameter, tool rotation speed and traverse speed, respectively. On the other hand, the lowest

efficiency can be seen for tool rotation speed and pipe thickness, traverse speed, and pipe's thickness, as well as pipe's thickness and diameter. After examining the importance and effectiveness of the parameters, the predicted model can be modified by removing the terms that do not have much effect, or in other words, the terms whose P value obtained from the analysis of variance is more than 0.1 [57]. A modified model is presented in the following equation:

$$\begin{aligned} \text{Strength (MPa)} = & 323.91 + 17.13U + 2.21T + 4.12D \\ & + 6.84V - 35.35U * U - 32.24T * T \\ & - 22.42D * D - 14.61V * V + 38.07U * D \\ & + 35.50U * V - 15.44T * V - 50.31D * V \end{aligned} \quad (7)$$

The results of the analysis of variance for the modified model are given in Table 6. According to Table 6, it is clear that after removing the low-impact terms, the P values obtained for the modified model for all terms are less than 0.1. The R^2 value decreases after modifying the model from 0.9347 to 0.9102, and the adjusted value of R^2 decreases from 0.8586 to 0.8332 after modifying the model. On the other hand, a P value less than 0.07 indicates that the model is very effective. In order to achieve a

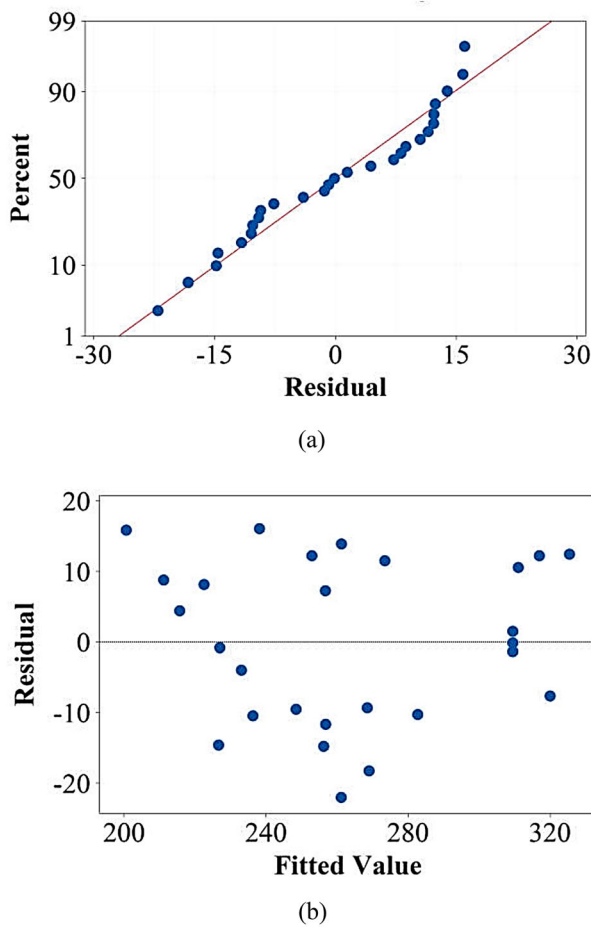
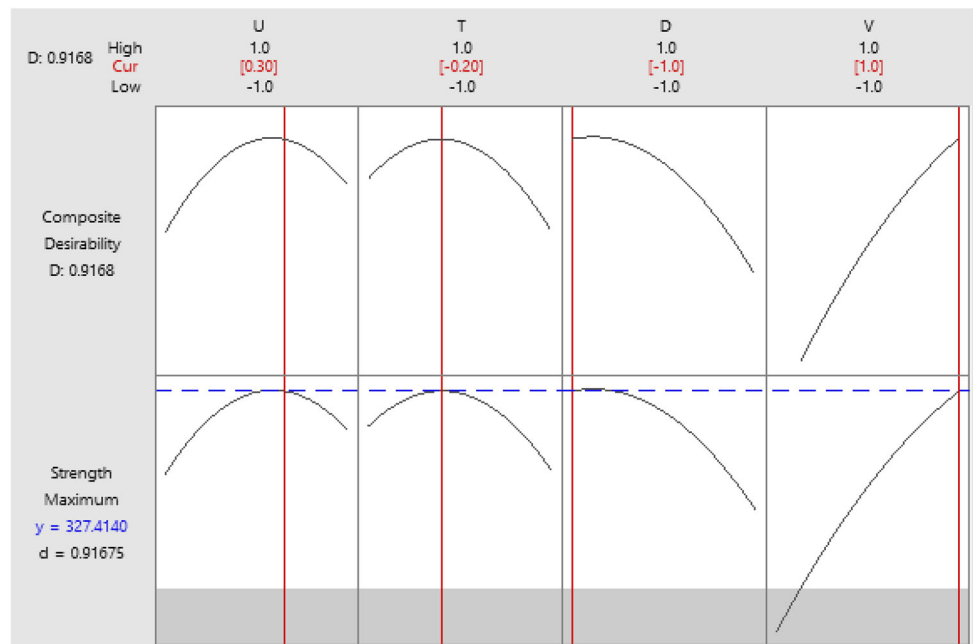


Fig. 5 **a** Normal plots of response residuals, **b** residuals versus fits plot

Fig. 6 Optimized parameters using desirability function

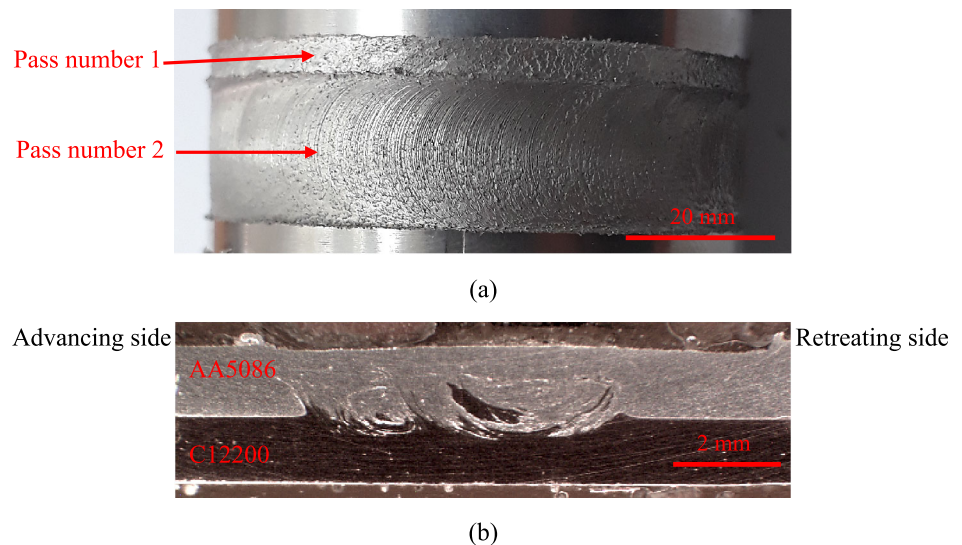
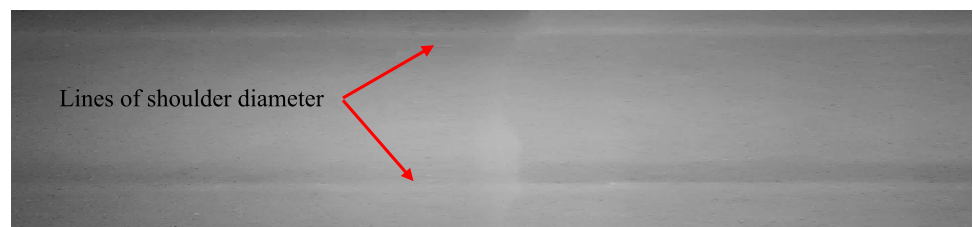


suitable model, it is necessary to check the accuracy of the model. According to Table 5, the predicted R^2 value is 0.6244, which shows the initial model’s ability to predict 62% of the response. Figure 5 shows the normal residual and error percentage diagrams for the modified model. It is observed that the residues form a horizontal band around the zero-line value while distributing randomly around this line. As shown in Fig. 5a, the proximity of points to the line indicates a small error in the model prediction. According to Table 6, the predicted R^2 value increases to 0.8896 after modifying the model, which indicates the 88% predictability of the model.

Due to the fact that the process was studied as a multi-response using the RSM, the responses should be optimized simultaneously. Derringer and Suich [58] expressed this optimization with the desirability function. Using this function, responses are expressed in a dimensionless manner between zero and one and are denoted by D . The number zero represents the lowest desirability and the number one represents the highest desirability. In this study, four parameters were optimized, and the degree of desirability between all is obtained using composite optimization. Figure 6 shows the predicted response using the desirability function. The vertical line inside each cell determines the optimal parameter settings, and the horizontal dash line determines the joint strength. The composite desirability of the parameters is $D = 0.9168$. This desirability in the parameters of rotational speed, traverse speed, pipe’s diameter, and pipe’s thickness being 660 rpm, 80 mm/min, 24 mm, and 1.4 mm, respectively,

Table 7 Comparison between measured and predicted results at optimum parameters

Experiment number	UTS (MPa)		
	Obtained	Predicted	Error
1	345.56	341.86	1.08%
2	349.32	341.86	2.18%
3	347.12	341.86	1.53%

Fig. 7 **a** Top of FSWed sample, and **b** cross section of FSWed sample with optimum parameters**Fig. 8** X-ray radiography result of FSWed samples with optimum parameters

has shown the joint strength of 341.86 MPa. In order to verify the optimal parameters estimated by the model, the welding process was performed experimentally by considering the optimal parameters, and the results are reported in Table 7. As can be seen, the average tensile strength measured from the experiment is 347.33 MPa, which is very close to the value estimated by the model.

The microstructural studies were performed on the cross section of the sample welded using the optimal parameter. Macro images of the upper surface, as well as the cross section of the two-layer pipe fabricated by the optimal parameter, are shown in Fig. 7. As can be seen, the cross section as well as the upper surface of the sample is free of common defects in the FSW process. As shown in Fig. 8, the welded samples are inspected by X-ray radiography. The results show that this sample does not contain any

defects. The cross section of the two-layer aluminum-copper pipe and microstructure of different zones are shown in Fig. 9. The SZ's microstructure contains equiaxed grains in both copper and aluminum side, which is formed according to [5, 48] due to dynamic recrystallization during stirring. The thermo-mechanically affected zone (TMAZ) consists of elongated grains that are stretched by the flow of material in the SZ, and dynamic recrystallization will not occur in this zone. This work has applied the scanning electron microscopy (SEM) and X-ray diffraction (XRD) approaches to perform a microstructural assessment and examine the intermetallic compounds that appear within the welding zone. The SEM results in the stir zone are provided in Fig. 10. Due to the plastic deformation and thermal history within the friction-stir process, Cu and Al blend in each other based on their flow behaviors

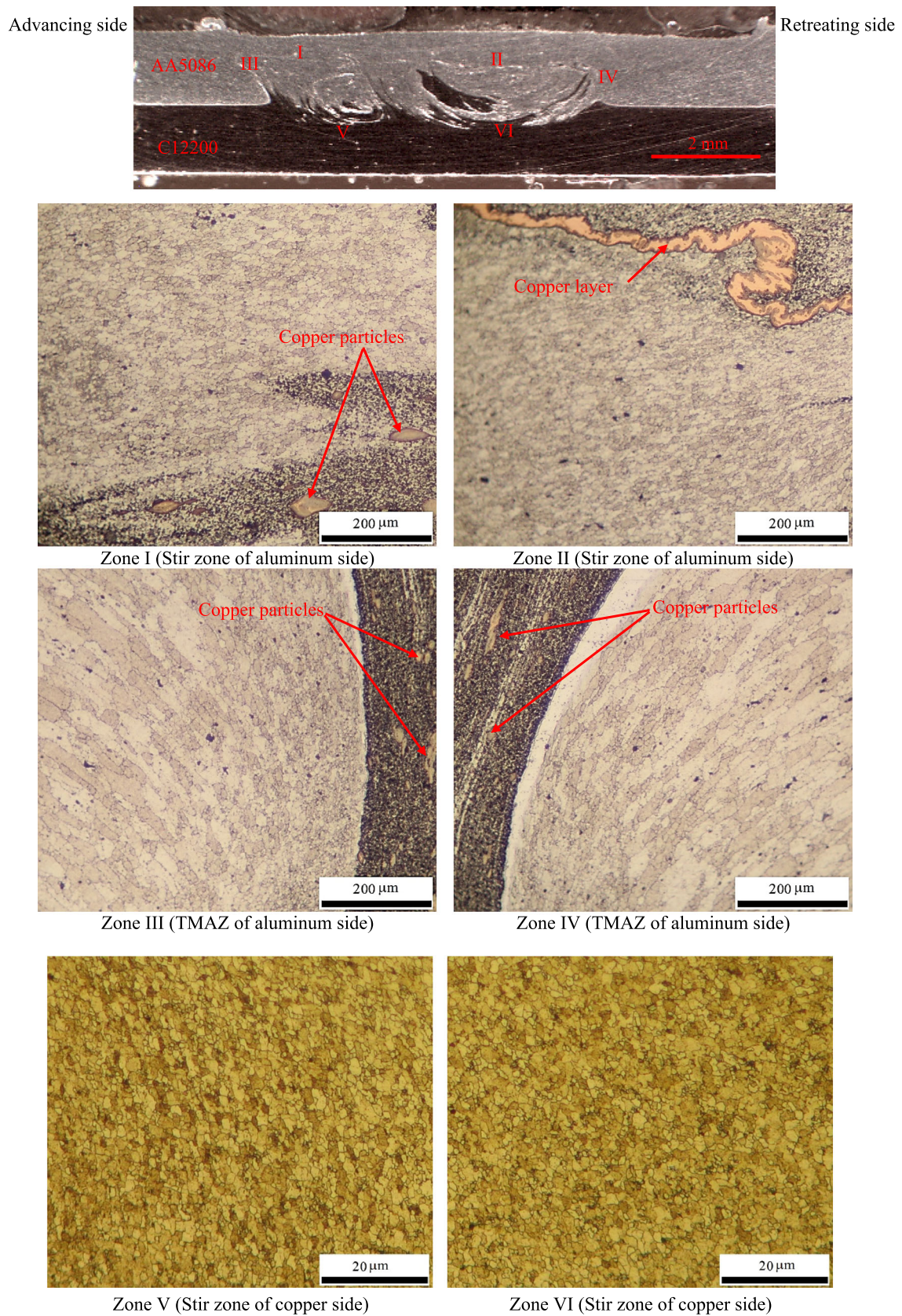


Fig. 9 Cross section of the two-layer aluminum–copper pipe fabricated with optimum parameters and microstructure of different zones

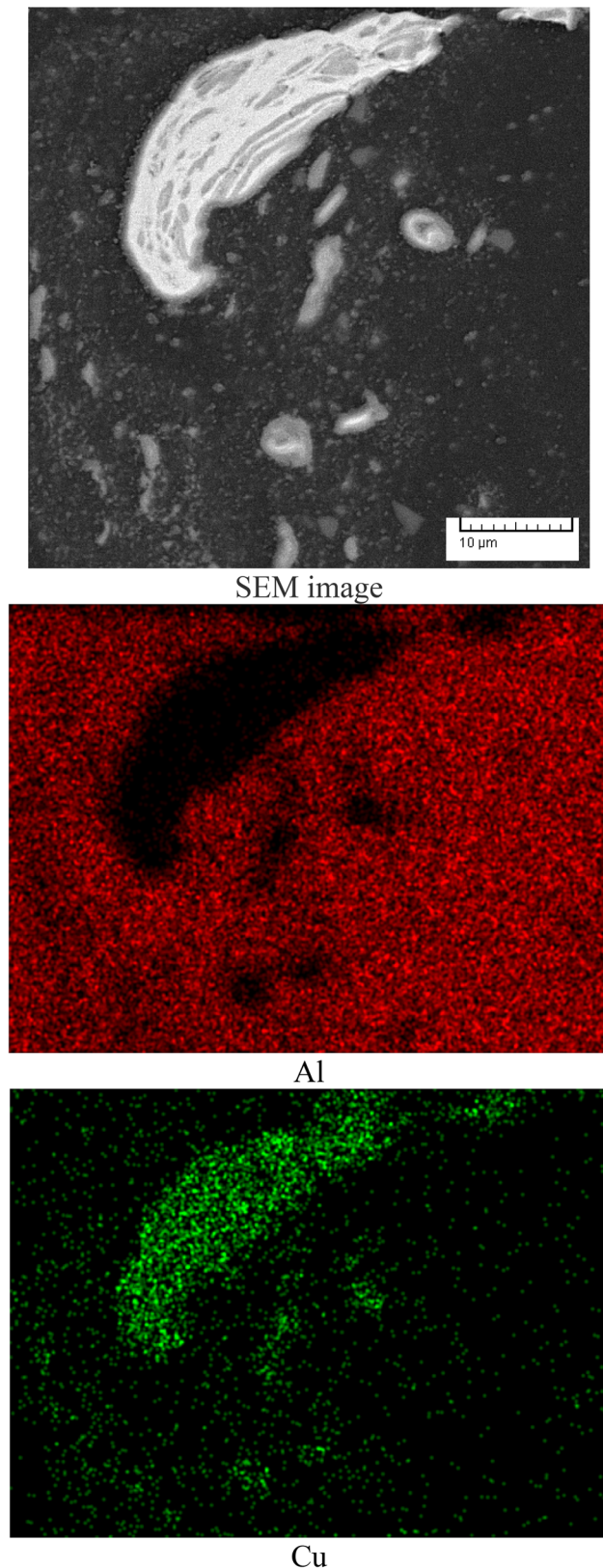


Fig. 10 SEM image and its corresponding EDS map analysis of an area on the center of stir zone

within the stir zone. Cu forms a layered structure within the Al matrix in the stir zone, even though Cu parts separate toward the stir zone, generating distinct Cu islands. This is attributed to the simultaneous contributions of material flow and heat that draw the Cu veins from the weld bottom toward the top of the stir zone. In a metallurgical sense, such layered sites represent suitable candidates for intermetallic compound generation. The XRD result is illustrated in Fig. 11 for the stir zone. According to Fig. 11, there are Cu, Al, and Cu–Al intermetallic compound (i.e., CuAl_2) in the stir zone. The Cu-rich particles of the stir zone were subjected to line scan analysis, as reported in Fig. 12. According to Fig. 12, there are large Cu and Al concentration in the Cu particle–Al matrix interface. This suggests that Al–Cu intermetallic compounds are generated within the stir zone. It is worth mentioning that friction stir welding subjects the stir zone to substantial plastic deformation. This could strongly raise the diffusion rate through the static state. Due to material deformation arising from traverse and rotational tool speeds, thin material layers form within the stir zone. As a result, one can say that Al–Cu intermetallic compounds are generated within the Cu particle–layer joints on account of the substantial temperature and plastic deformation within the stir zone.

5 Conclusions

The effect of friction stir welding process parameters and geometrical parameters of pipe in the fabrication of two-layer AA5086–C12200 pipe was studied using Box–Behnken design of response surface methodology. The main findings of this research are as follows:

- By increasing the thickness and diameter of the pipe to 2 mm and 64 mm, respectively, the joint strength decreases.
- To express the interaction of the parameters, the maximum effectiveness is for traverse speed and pipe diameter, tool rotation speed and pipe diameter, tool rotation speed and traverse speed, respectively. On the other hand, the lowest efficiency can be seen for tool rotation speed, and pipe's thickness, traverse speed, and pipe thickness, as well as pipe thickness and diameter.
- The composite desirability of the parameters is $D = 0.9168$. Also, the optimum rotational speed, traverse speed, pipe diameter, and pipe thickness are 660 rpm, 80 mm/min, 24 mm, and 1.4 mm, respectively. The maximum predicted and measured joint strength at optimum parameters are 341.86 and 347.33 MPa, respectively.

Fig. 11 X-ray diffraction of the stir zone

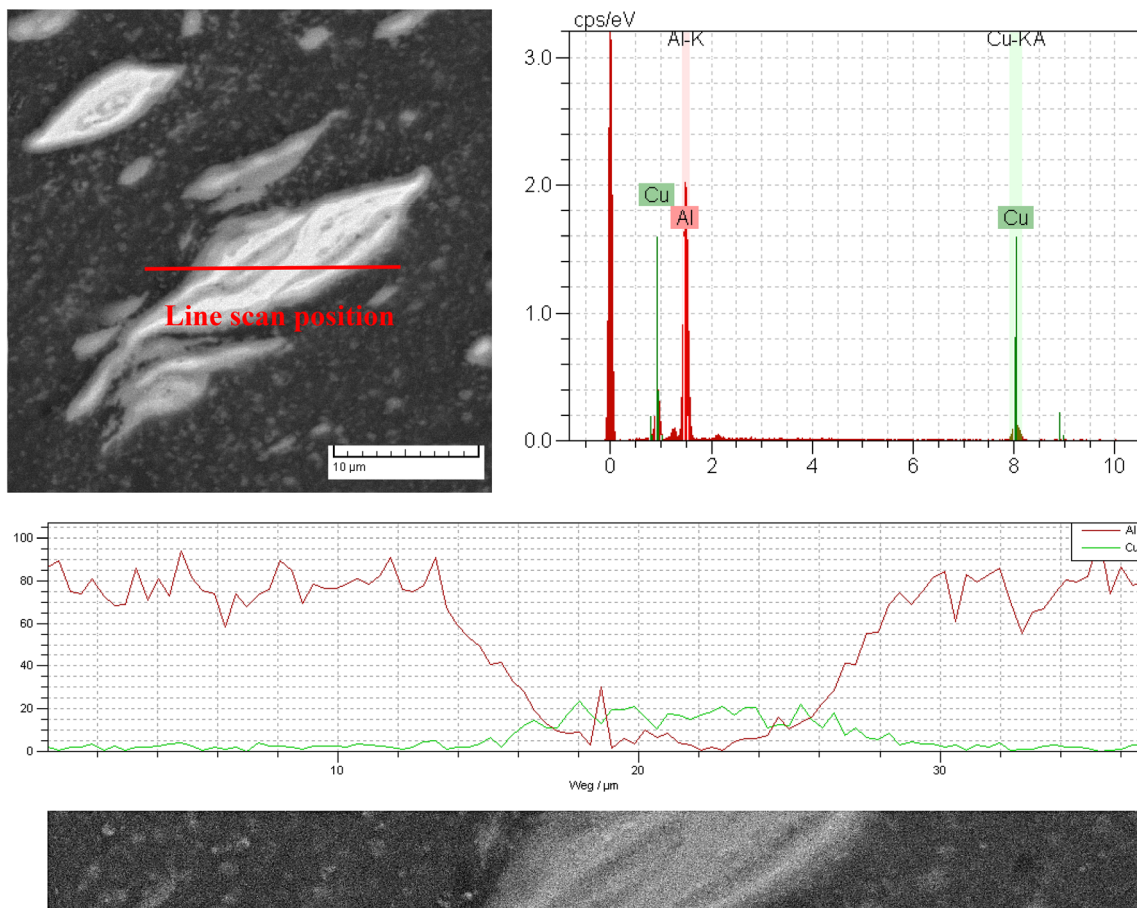
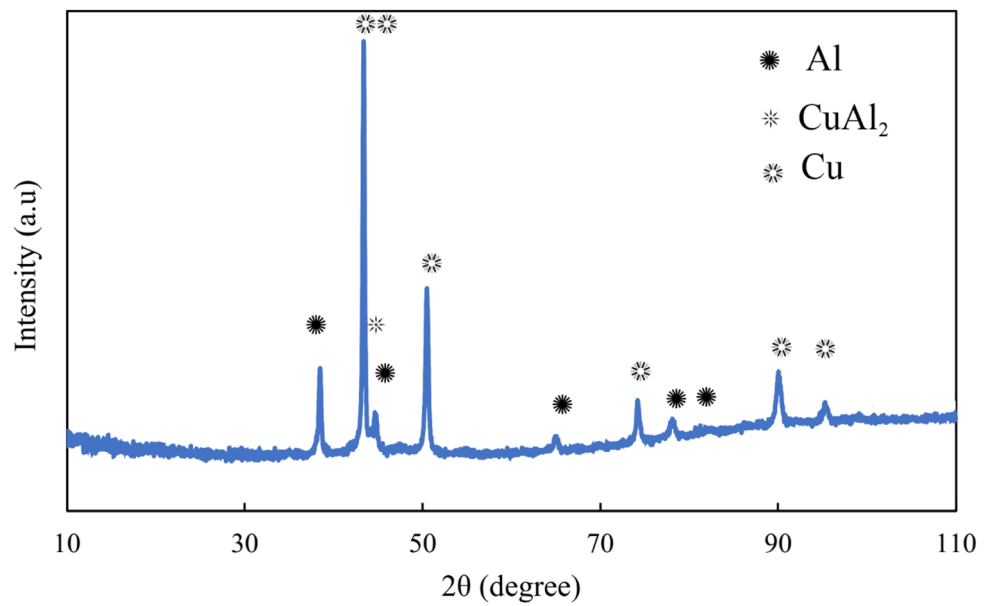


Fig. 12 Line scan analysis from the copper rich particles present in the stir zone

- By simultaneous decrease in rotational speed and pipe thickness, the joint strength decreases. By increasing the rotational speed and decreasing the pipe diameter, the joint strength decreases. Also, by increasing the rotational speed and decreasing the traverse speed, the joint strength decreases.

- In both the minimum and maximum diameter of the pipe, if the thickness of the pipe decreases or increases from the middle value (1.5 mm), the joint strength decreases. Maximum joint strength is obtained when the middle value of thickness (1.5 mm) and diameter (44 mm) are selected.
- It is observed that when the traverse speed and the diameter of the pipe increase or decrease simultaneously, the joint strength decreases, and also similar results can be seen when the traverse speed and the thickness of the pipe decrease or increase at the same time.

Author Contributions MFN took part in investigation, resources, writing—original draft. ME involved in conceptualization, methodology, writing—review & editing, supervision. HJA participated in conceptualization, methodology, writing—review & editing, supervision. MJM took part in conceptualization, methodology, writing—review & editing, supervision.

Funding This research was sponsored by the Babol Noshirvani University of Technology.

Data Availability The manuscript has no associated data, or the data will not be deposited.

Declarations

Conflict of interest The authors declare that they have no competing interests.

Ethical Approval This paper is new. Neither the entire paper nor any part of its content has been published or has been accepted elsewhere. It is not submitted to any other journal as well.

References

- Martinsen K, Hu S, and Carlson B, *CIRP Ann* **64** (2015) 679.
- Abd Elnabi M M, Abdel-Mottaleb M, Osman T, and Mokadem El A, *J Mater Res Technol* **8** (2019) 1684.
- Tavassolimanesh A, and Nia A A, *J Alloys Compd* **751** (2018) 299.
- Moradi M M, Jamshidi Aval H, and Jamaati R, *Modares Mech Eng* **16** (2016) 394.
- Kah P, Vimalraj C, Martikainen J, and Suoranta R, *Int J Mech Mater Eng* **10** (2015) 1.
- Mirjalili A, Serajzadeh S, Jamshidi Aval H, and Kokabi A, *Mater Manuf Process* **28** (2013) 683.
- Eskandari M, Aval H J, and Jamaati R, *J Manuf Process* **41** (2019) 168.
- Mishra R S, and Ma Z, *Mater Sci Eng R Rep* **50** (2005) 1.
- Golafshani K B, Nourouzi S, and Jamshidi Aval H, *Mater Sci Technol* **35** (2019) 1061.
- Cai W, Daehn G, Vivek A, Li J, Khan H, Mishra R S, and Komarasamy M, *J Manuf Sci Eng* **141** (2019) 031012.
- Li W, and Patel V, *Solid State Welding for Fabricating Metallic Parts and Structures* (2020).
- Khojastehnezhad V M, and Pourasl H H, *Trans Nonferr Met Soc China* **28** (2018) 415.
- Thomas W, and Nicholas E, *Mater Des* **18** (1997) 269.
- Campo K N, Campanelli L C, Bergmann L, dos Santos J F, and Bolfarini C, *Mater Des (1980–2015)* **56** (2014) 139.
- Barekatin H, Kazeminezhad M, and Kokabi A, *J Mater Sci Technol* **30** (2014) 826.
- Argesi F B, Shamsipur A, and Mirsalehi S E, *Acta Metall Sin (English Letters)* **31** (2018) 1183.
- Celik S, and Cakir R, *Metals* **6** (2016) 133.
- Liu P, Shi Q, Wang W, Wang X, and Zhang Z, *Mater Lett* **62** (2008) 4106.
- Galvao I, Oliveira J, Loureiro A, and Rodrigues D, *Sci Technol Weld Join* **16** (2011) 681.
- Galvão I, Leitão C, Loureiro A, and Rodrigues D, *Soldag Inspeção* **17** (2012) 02.
- Galvão I, Verdera D, Gesto D, Loureiro A, and Rodrigues D, *J Mater Process Technol* **213** (2013) 1920.
- Ebrahimzadeh V, Paidar M, Safarkhanian M, and Ojo O O, *Int J Adv Manuf Technol* **96** (2018) 1237.
- Gerçekcioglu E, Eren T, Yildizli K, Kahraman N, and Salamci E, *J Balk Tribol Assoc* **12** (2006) 24.
- Doos Q M, and Wahab B A, *Int J Mech Eng Robot Res* **1** (2012) 143.
- Duan R, Xie G, Luo Z, Xue P, Wang C, Misra R, and Wang G, *Mater Sci Eng A* **791** (2020) 139620.
- Giorjão R A R, Pereira V F, Terada M, da Fonseca E B, Marinho R R, Garcia D M, and Tschiptschin A P, *J Mater Res Technol* **8** (2019) 243.
- Ronevich J A, Somerday B P, and Feng Z, *Int J Hydrog Energy* **42** (2017) 4259.
- Naqibi M F, Elyasi M, Aval H J, and Mirnia M J, *Trans Indian Inst Met* **74** (2021) 285.
- Jamshidi Aval H, and Falahati Naghibi M, *Sci Technol Weld Join* **22** (2017) 562.
- Li W, Wen Q, Yang X, Wang Y, Gao D, and Wang W, *Mater Des* **134** (2017) 383.
- Tavassolimanesh A, and Nia A A, *J Manuf Process* **30** (2017) 374.
- Lakshminarayanan A, and Balasubramanian V, *Trans Nonferr Met Soc China* **18** (2008) 548.
- Salehi M, Saadatmand M, and Mohandesi J A, *Trans Nonferr Met Soc China* **22** (2012) 1055.
- Lakshminarayanan A, and Balasubramanian V, *Trans Nonferr Met Soc China* **19** (2009) 9.
- Heidarzadeh A, Barenji R V, Khalili V, and Güleriyüz G, *Vacuum* **159** (2019) 152.
- Dharmalingam S, and Lenin K, *Mater Today Proc* (2020).
- Gill A, Dhiman D P, Gulati V, and Sharma S, *Mater Today Proc* **5** (2018) 27865.
- Khan N, *Mater Today Proc* **29** (2020) 448.
- Kumar S S, Murugan N, and Ramachandran K, *Measurement* **137** (2019) 257.
- Palanivel R, Mathews P K, and Murugan N, *J Cent South Univ* **20** (2013) 2929.
- Mohamadigangaraj J, Nourouzi S, and Aval H J, *Measurement* **165** (2020) 108166.
- Dean A, Voss D, and Draguljić D, in *Design and Analysis of Experiments*, Springer (2017), pp 565–614.
- Senthil S, Parameshwaran R, Nathan S R, Kumar M B, and Deepandurai K, *Struct Multidisc Optim* **62** (2020) 1117.
- El-Kassas A, and Sabry I, *Int J Appl Eng Res* **14** (2019) 4562.
- Wang H, Bouchard R, Eagleson R, Martin P, and Tyson W R, *J Test Eval* **30** (2002) 382.
- Montgomery D C, *Montgomery Design and Analysis of Experiments* Eighth Edition. Arizona State University, Copyright, 2009 (2013) 2001.

47. Kim Y G, Fujii H, Tsumura T, Komazaki T, and Nakata K, *Mater Sci Eng A* **415** (2006) 250.
48. Podržaj P, Jerman B, and Klobčar D, *Metalurgija* **54** (2015) 387.
49. Kah P, Rajan R, Martikainen J, and Suoranta R, *Int J Mech Mater Eng* **10** (2015) 1.
50. Arbegast W J, *Hot Deform Alum Alloys III* (2003) 313.
51. Safi S V, Amirabadi H, and Kazem M B G, *Mech Mater Sci Eng J* (2016).
52. Beygi R, Mehrizi M Z, Verdera D, and Loureiro A, *J Mater Process Technol* **255** (2018) 739.
53. Sharma N, and Siddiquee A N, *Trans Nonferr Met Soc China* **27** (2017) 2113.
54. Khodir S, Ahmed M, Ahmed E, Mohamed S M, and Abdel-Aleem H, *J Mater Eng Perform* **25** (2016) 4637.
55. Karthikeyan R, and Balasubramanian V, *Int J Adv Manuf Technol* **51** (2010) 173.
56. Khuri A I, and Cornell J A, *Response Surfaces: Designs and Analyses*, Routledge (2018).
57. Sundaram M, and Visvalingam B, *J Weld Join* **34** (2016) 23.
58. Derringer G, and Suich R, *J Qual Technol* **12** (1980) 214.

Publisher's Note Springer Nature remains neutral with regard to jurisdictional claims in published maps and institutional affiliations.